ORIGINAL ARTICLE

Spatial variation in specific leaf area and horizontal distribution of leaf area in juvenile western larch (*Larix occidentalis* Nutt.)

G. M. Williams[1,2] · A. S. Nelson[1]

Abstract

Key message **Models were developed to predict spatial distribution of specific leaf area (SLA) and horizontal distribution of leaf area for western larch. Cardinal branch direction significantly influenced both SLA and horizontal leaf area distributions.**

Abstract Leaf area, specific leaf area (SLA), and their spatial distribution in the crown are important indicators of biological response to changes in growing conditions including light and water availability. Western larch (*Larix occidentalis* Nutt.) is a deciduous coniferous pioneer species in the U.S. Inland Northwest known for its rapid growth, high-quality wood, and ecological importance. Analysis with nonlinear models revealed that SLA and horizontal leaf area distributions differ between cardinal quadrants of juvenile western larch crowns. SLA was significantly higher in the more illuminated, southern side of the crown, and leaf area peaked closer to the stem in the southwest quadrant. Similar to other conifers, horizontal distributions of foliage in western larch also shifted further outward towards the branch tips with increasing depth in the crown. Models developed for horizontal distribution of leaf area and spatial distribution of specific leaf area for western larch may be extended by future researchers to predict its response to environmental variables or management practices.

Keywords Biomass · Shade intolerance · Probability density function · Nonlinear mixed-effects model · Inland Northwest · Leaf economics · Morphological plasticity

Introduction

Photosynthetic productivity of trees depends on water, light availability, and the distribution of leaf area within the canopy, including its horizontal distribution along branches

✉ G. M. Williams
will1809@purdue.edu

A. S. Nelson
asnelson@uidaho.edu

1 Department of Forest, Rangeland and Fire Science, University of Idaho, Moscow, ID 83844, USA

2 Present Address: Hardwood Tree Improvement and Regeneration Center, Department of Forestry and Natural Resources, Purdue University, West Lafayette, IN 47907, USA

(Horn 1971; Stenberg et al. 1993). Deeper within the crown from both vertical and horizontal directions, photosynthetically active radiation available to foliage diminishes (Stenberg et al. 1994). The size of gaps between trees in a stand and the amount of resulting side shade are major determinants of light interception. In turn, horizontal distribution of foliage and lateral branch growth feedback on each other during canopy closure (Oliver and Larson 1990). Depending on the shade tolerance of a species, these processes can have lasting influences on stand dynamics and future stand structure.

Leaf area (LA) and foliar mass (FM) differ in their distributions within the crown; their relative distributions can be related to one another through spatial variation in specific leaf area (SLA), the ratio of projected area to dry biomass. Sun-leaves tend to have higher FM, lower LA, and therefore, lower SLA than shade leaves. SLA is positively correlated with net photosynthesis on a leaf mass basis (Jurik 1986; Oren et al. 1986; Ellsworth and Reich 1993; Reich et al. 1997). SLA is generally higher for shade-tolerant species than shade-intolerant species, and has been observed to

decrease with increasing light availability (Niinemets and Kull 1994, 1995; Niinemets 1996; Temesgen and Weiskittel 2006; Perrin and Mitchell 2013). The amount and components of SLA variance differ between species (Marshall and Monserud 2003; Goudie et al. 2016), with greater variance across light gradients reported for shade-tolerant relative to shade-intolerant species (Chen et al. 1996; Bond et al. 1999). SLA also decreases as leaves age and is negatively correlated with leaf lifespan (Gulmon and Chu 1981; Chabot and Hicks 1982; Reich et al. 1997; Ishii et al. 2002; Temesgen and Weiskittel 2006; Weiskittel et al. 2008).

In addition to light availability, hydraulic factors are thought to underpin spatial variation in SLA. Functional limitation of SLA due to lower turgor pressure during initial leaf expansion is the basis for the hydraulic resistance and gravitational water potential hypotheses to explain observations of decreasing SLA with longer paths traveled by water to developing foliage (Tardieu et al. 1999; Phillips and Riha 1993; Ibrahim et al. 1998; Myers et al. 1998; Marshall and Monserud 2003). Under this hypothetical framework, the degree of variation in SLA should also depend on stomatal conductance, which is more strongly linked to vapor deficit in some species, and stem water potential in others (Anfodillo et al. 1998).

Western larch (*Larix occidentalis* Nutt.) is a shade-intolerant pioneer, and unique among mid-elevation conifers of the U.S. Inland Northwest (INW) for its deciduous habit. As an important provider of wildlife habitat (McClelland et al. 1979) and the fastest growing and most fire-adapted species in the region (Schmidt and Shearer 1990), *L. occidentalis* is worthy of focus for research to improve management strategies. Due to past and projected declines precipitated by fire suppression (Arno et al. 1997) and climate change (Rehfeldt and Jaquish 2010), *L. occidentalis* has also been targeted by public-sector restoration efforts (Scott et al. 2013). While *L. occidentalis* has an advantage on disturbed sites due to high photosynthetic rate per unit mass of high-SLA foliage and sustained stomatal conductance through the growing season (Higgins et al. 1987), it suffers during stand competition. Vertical distribution of foliar biomass was recently modeled across a large portion of the range of *L. occidentalis* (Williams et al. 2017). Side-shade is an important factor during stand competition (Oliver and Larson 1990). Thus, plasticity of horizontal distribution of leaf area is an important component in the adaptive response to stand competition.

Studies of other species have used probability density functions (PDFs) to model horizontal foliage distributions (Wang et al. 1990; Stenberg et al. 1993; Kershaw and Maguire 1996; Xu and Harrington 1998; Temesgen et al. 2003), and fixed and mixed effects models to describe spatial variation of SLA within the crown (Ishii et al. 2002; Marshall and Monserud 2003; Temesgen and Weiskittel 2006; Weiskittel et al. 2008; Fellner et al. 2016). In most species, horizontal distribution of foliage depends on vertical branch position in the crown and the total crown length (Stenberg et al. 1993; Kershaw and Maguire 1996; Xu and Harrington 1998; Temesgen et al. 2003). Development of baseline empirical leaf area and SLA distribution models can also provide a framework for future research investigating the response of *L. occidentalis* to extrinsic variables such as management, natural disturbance, and climate change (Buckley et al. 1997).

We employed a multilevel modeling approach to identify the major intrinsic components of variance of SLA and horizontal leaf area distribution in crowns of juvenile *L. occidentalis*. The specific objectives of the study were: (A) to develop spatial models of SLA as functions of intrinsic variables such as horizontal position along the branch, vertical position and dimensions of the branch, tree-level measurements, and random effects to account for extrinsic factors; (B) to model the horizontal distribution of leaf area along individual branches; and (C) to model parameter estimates for PDFs fit to horizontal leaf area to identify which intrinsic variables significantly influence the horizontal distribution of leaf area along branches, and to model how the distribution responds to those variables.

Materials and methods

Study site and data collection

A total of 15 juvenile *L. occidentalis* trees were destructively sampled from 4 locations in Latah County of northern Idaho between June 29 and August 11 of 2016 during the peak of foliage development in summer. Mean annual temperature of the sites ranged from 7.7 to 8.8 °C and mean annual precipitation ranged from 658 to 688 mm. Elevation ranged from 957 to 1330 m a.s.l. Latitude ranged from 46°49′48″N to 47°6′36″N. Age of the trees ranged from 10- to 14-years-old. All stands were naturally regenerated using seed-tree harvests with western larch as the preferred species left as the seed-trees. Once the stands were well-stocked with western larch seedlings [~ 1200 trees per hectare (1.8 × 1.8 m spacing)], the residual seed-trees were removed. No further management occurred within the stands until they were thinned to 741 trees per hectare [3.6 × 3.6 m spacing] the year the trees were sampled for the study. Between 2 and 6 trees were sampled from each site.

For every tree at each location, diameter at breast height (DBH), diameter at the base of the live crown (DBLC), height (TH), and vertical distance along the stem from the base of the stem to the base of the live crown (HBLC) were recorded (Table 1). For every branch on every tree, length from tip to stem junction (TBL), vertical distance along the stem from the base of the crown to the center of the junction

Table 1 Summary of trees destructively harvested for leaf area study

Site	n	DBH (mm)			DBLC (mm)			TH (cm)			HBLC (cm)		
		Min	Mean	Max	Min	Mean	Max	Min	Mean	Max	Min	Mean	Max
Carsc	6	61.0	115.6	162.6	71.1	149.9	246.4	652.3	943.9	1137.0	18.3	64.5	100.6
TMU	3	76.2	125.3	188.0	76.2	125.3	188.0	810.8	1079.0	1277.0	137.2	149.4	161.5
UI217	4	96.5	137.2	177.8	99.1	141.0	167.6	816.9	1058.4	1295.0	57.9	150.1	240.8
UI486	2	73.7	101.6	129.5	71.1	100.3	129.5	762.0	1011.9	1262.0	128.0	169.2	210.3

See Table 3 for definitions of variable abbreviations

(HIC), and diameter 5 cm from the junction (BD) were recorded (Table 2). The distance from the stem junction to the start of foliage (DTF) and the cardinal quadrant of the branch (NE, SE, SW, and NW) was also recorded. The main stem of each tree and all attached branches were divided into three equal vertical sections along the stem. Within each section of each tree, two random branches were selected for measurement of foliar biomass (FM), with the exception of a single tree in the data set for which only 4 branches were sampled in the crown for foliage (Carsc 6, see Table 2). Each selected branch was divided into 10-centimeter horizontal segments along its length, and FM was measured separately for each segment (Online Resource 1).

For leaf area analysis, initial measures of LA and SLA for each 10 cm segment revealed that SLA varied across the branch, but was consistently similar within 20–30 cm horizontal sections. Thus, to minimize processing time, 3 or 4 horizontal segments were randomly selected from each of the six branches measured for FM per tree as subsamples for SLA analysis. A subsample of approximately 50–100 needles were taken from each of the branch segments selected for LA analysis. Any remaining foliage from the branch segments selected for leaf area analysis were processed along with the rest of the branch segments for foliage biomass. Each needle SLA subsample was scanned and analyzed for projected one-sided area with WinSEEDLE™ (Regent Instruments Inc., Quebec CA) at the 800 dpi setting. The dry biomass of each needle subsample was processed separately from any remaining foliage from its corresponding branch segment to estimate SLA.

Foliage from the rest of the branch segments, from the needle LA subsamples and from the remainder of the segments from which the LA subsamples were taken were placed in an oven and allowed to dry for at least 72 h at 65 °C. Foliage was then removed from each segment and weighed on a balance to the nearest 0.1 mg. LA from subsamples were divided by their FM to obtain SLA values for the subsampled branch segments.

Specific leaf area models

SLA values calculated for sampled segments (Online Resource 2) were used to fit linear and nonlinear models of a variety of forms to estimate SLA across the crown as a

Table 2 Summary of branches harvested for leaf area study

Site	Tree	n	BD (mm)			HIC (cm)			TBL (cm)		
			Min	Mean	Max	Min	Mean	Max	Min	Mean	Max
Carsc	1	6	5	8	11	134	402	647	71	125	161
Carsc	2	6	5	13	24	159	437	735	56	149	212
Carsc	3	6	8	11	15	143	493	762	88	146	172
Carsc	4	6	4	6	12	52	287	512	36	69	107
Carsc	5	6	7	15	24	128	502	872	67	142	237
Carsc	6	4	6	8	10	351	509	653	59	90	128
TMU	1	6	4	9	14	147	506	848	37	86	120
TMU	2	6	9	15	18	177	585	957	83	143	173
TMU	3	6	4	9	14	73	322	549	50	87	115
UI217	1	6	9	13	19	55	503	887	93	137	199
UI217	2	6	6	10	14	134	341	552	90	120	148
UI217	3	6	8	11	14	195	422	619	91	127	172
UI217	4	6	5	14	21	274	548	856	52	152	227
UI486	1	6	5	7	9	91	302	485	54	92	120
UI486	2	6	5	11	17	229	544	857	49	123	174

See Table 3 for definitions of variable abbreviations

function of an array of variables including vertical branch position (i.e., HIC, DIC, RHIC, or RDIC), horizontal position of the foliage along the branch (i.e., DAB, PAB, RDAB, RPAB, DAF, RPAF, or RDAF), and other branch and tree-level measurements (Table 3).

Variation due to unmeasured tree-level factors such as age and extrinsic variables such as social position were accounted for by including random effects for site and tree within site. Models were fit and parameter estimates obtained by maximum likelihood estimation with the "nlme" function in the "nlme" package of R (Core Team 2017; Pinheiro et al. 2017), which allows the incorporation of hierarchical random effects and the ability to account for autocorrelation and unequal variance. Starting parameter values specified in the "nlme" function were obtained from the "proc model" function in SAS (SAS Institute Inc. 2016).

Parameter estimates were screened for significance using a threshold *p* value of 5%, and non-significant parameters were considered to be zero and excluded from the model. Once a set of models with all significant parameters was obtained, the relative explanatory power, or goodness of fit of the models was assessed using multiple selection criteria: likelihood ratio tests, adjusted and generalized R^2, Akaike information criterion (AIC), and root mean squared error (RMSE). During model building, the simplest model that yielded a statistically significant improvement in a likelihood ratio test over a corresponding base model with one less parameter was selected and retained. This process was repeated until no significant improvement in fit was obtained from the inclusion of additional variables. The final model retained was used to estimate leaf area of individual horizontal segments.

Table 3 Variables to be tested in model fitting

Variable	Definition	Formula
Segment		
DAB (cm)	Distance along branch, distally from stem junction	
PAB (cm)	Distance along branch, proximally from branch tip	TBL − DAB
RDAB	Relative distal distance along branch from stem	DAB/TBL
RPAB	Relative proximal distance along branch from tip	PAB/TBL
DAF (cm)	Distal distance from start of foliage toward tip	DAB − DTF
RPAF	Relative proximal distance along foliated portion	PAB/FL
RDAF	Relative distal distance along foliated portion	DAF/FL
FM (g)	Foliar biomass of branch segment	
LA (cm^2)	Leaf area of branch segment	
SLA (cm^2 g^{-1})	Specific leaf area of branch segment	LA/FM
Branch		
ω_{ij} (Tree)	Random effect of tree (j) within site (i) on branch	
BD (mm)	Branch diameter at stem junction	
DTF (cm)	Distance from stem junction to start of foliage	TBL − FL
FL (cm)	Length of foliated portion of branch	
TBL (cm)	Branch length	
NW, NE, SW, and SE	Cardinal quadrant of branch	Dummy variable (equal 1 or 0)
HIC (cm)	Height into crown from crown base	
DIC (cm)	Depth into crown from stem apex	CL − HIC
RHIC	Relative height into crown from base	HIC/CL
RDIC	Relative depth into crown from apex	DIC/CL
Tree		
φ_i (Site)	Random effect of site location (i) on tree	
TH (cm)	Tree height	
HBLC (cm)	Height to base of crown	
CL (cm)	Length of the crown	TH − HBLC
DBLC (mm)	Diameter of stem at base of crown	
DBH (mm)	Diameter at breast height (@1.3 m)	
HMC (cm)	Height to the midpoint of the crown	HBLC + CL/2

Horizontal distribution of leaf area along branches

Data representing the horizontal distribution of leaf area along branches was obtained by estimating SLA for each branch segment with the SLA model and multiplying by the foliar mass measured for each segment on 88 branches from 15 trees (Online Resource 1). The left- and right-truncated Weibull (Eq. 1), β-distribution (Eq. 2), and Johnson's S_B (Eq. 3) functions were fit to the LA distribution along individual branches and parameters recovered using maximum likelihood estimation (Weiskittel et al. 2009). The forms of the PDFs are expressed as

$$p(X) = \frac{\beta X^{\beta-1} e^{-((X/\eta)^\beta - (\gamma/\eta)^\beta)}}{\eta^\beta}, \tag{1}$$

$$p(X) = \frac{X^c(1-X)^{d-1}}{\Gamma(c)\Gamma(d)/\Gamma(c+d)}, \tag{2}$$

$$p(X) = \frac{\tau e^{-\frac{1}{2}\left(\psi + \tau \ln \frac{X}{1-X}\right)^2}}{\sqrt{2\pi} X(1-X)}, \tag{3}$$

where X represents the horizontal position along the branch and $p(X)$ is the relative leaf area density at that position, such that $p(X)dX$ is the proportion of total branch leaf area over an interval dX. Relative proximal distance from branch tip to the stem (RPAB, Table 3) was used for X to facilitate comparison across branches and trees of different size, to permit comparison to past studies, and because it reflects light attenuation in the crown. In the Weibull function (Eq. 1), β is the skew (shape) parameter, η is the kurtosis (scale) parameter, and γ is the truncation point. In the β-distribution (Eq. 2), c and d are shape parameters, and $\Gamma(x)$ is the gamma function. In Johnson's S_B (Eq. 3), ψ and τ are shape parameters.

To make the discrete data more amenable to fitting PDFs, LA estimates were divided into horizontal bins of equal length along the branch. The distribution of residuals and overall average root mean squared error (RMSE) and mean absolute bias (MAB) were compared among models and binning schemes to select the best model and number of bins. To assess model performance, the horizontal distribution of standard error and bias averaged for each bin across branch length was plotted to look for correlation. Once binning was optimized and the best-fitting PDF was selected, parameter estimates (i.e., Weibull η and β) recovered for individual branches were modeled as linear and nonlinear functions of branch and tree variables to analyze how the horizontal foliage distribution changes with respect to intrinsic factors. Model fitting was performed with the "nlme" package of

R (Core Team 2017; Pinheiro et al. 2017), using starting parameters obtained from "proc model" in SAS (SAS Institute Inc. 2016). Model building proceeded using the same bottom-up approach as in the specific leaf area models.

Results

Specific leaf area model

The young *L. occidentalis* trees in this study had an overall mean SLA of 64.22 ± 17.65 cm^2 g^{-1} and ranged from 15.62 to 131.92 cm^2 g^{-1} across branches, trees, and sites (Online Resource 2).

A total of 65 model forms were tested and compared for SLA of the 10 cm branch segments, and 12 additional models obtained by substituting initial slope parameter estimates as constants were also tested to allow for non-significance of the initial slope parameter estimates in model comparisons (Online Resource 3). Of the total 77 models, a mixed power and exponential function of HIC, HMC, RDAF, with dummy variables for SE and SW (Eq. 7 in Online Resource 3) had the highest likelihood, lowest AIC, and RMSE, and highest generalized and adjusted R^2 for combined fixed and random effects, but had 0.025 lower R^2 for fixed effects than the model with the highest R^2 for fixed effects (Eq. 9 in Online Resource 3).

However, a model substituting RPAB for RDAF (Eq. 8 in Online Resource 3) had comparable scores for all goodness of fit criteria with Eq. (7). RPAB was used because distance along the entire branch from the tip is more biologically informative in terms of light availability and the unfoliated portion of most branches was short. Use of RPAB also maintains consistency with the horizontal leaf area PDFs (Eqs. 1–3). Equation (4), which matched Eq. (8), but retained the non-significant initial slope parameter (m_0, Table 4), was selected and had the form.

$$\text{SLA} = m_0 \, \text{HIC}^{\,m_1 + \varphi_i + \omega_{ij}} \, \text{HMC}^{\,m_2 + m_3 RPAB + q_0(\text{SE} + \text{SW})} \tag{4}$$

where m_0, m_1, m_2, m_3, and q_0 are parameters (Table 4), φ_i and ω_{ij} are random effects for site i and tree j within site i on HIC, and SE and SW are dummy variables (0 or 1) for branches in the southeast and southwest quadrants, respectively. The inclusion of a factor for whether the branches were on the south side of the tree significantly improved the model fit over a base model that did not account for cardinal branch direction (Eq. 22 vs. Eq. 30 in Online Resource 3; $\chi^2 = 5.61$; $df = 1$; $0.01 < p < 0.025$). Overall, SLA had an inverse relationship with HMC and HIC, and was positively correlated with RPAB. The southern quadrants (SW and SE) had higher SLA after accounting for other variables (Fig. 1; Table 4).

Table 4 Parameter estimates for spatial SLA model

Model	Parameter	Estimate	SE fixed[a]	SD random (site)[b]	SD random (tree)[c]	p
SLA (Eq. 4)	m_0	2634.115	2022.226	NA[d]	NA	0.193
	m_1	− 0.237	0.013	0.144	0.020	0.000
	m_2	− 0.381	0.122	NA	NA	0.002
	m_3	0.022	0.003	NA	NA	0.000
	q_0	0.005	0.002	NA	NA	0.019

[a]Standard error for fixed effects

[b]Standard deviation for random effects for site

[c]Standard deviation for random effects for tree within site

[d]Parameter did not include random effects

Fig. 1 Specific leaf area predicted by Eq. 4 by quartile (25, 50 and 75%) of relative distance from tip to bole (RPAB), height to the middle of the crown (HMC), height of the branch from crown base (HIC), and whether the branch is on the south or north side of the crown
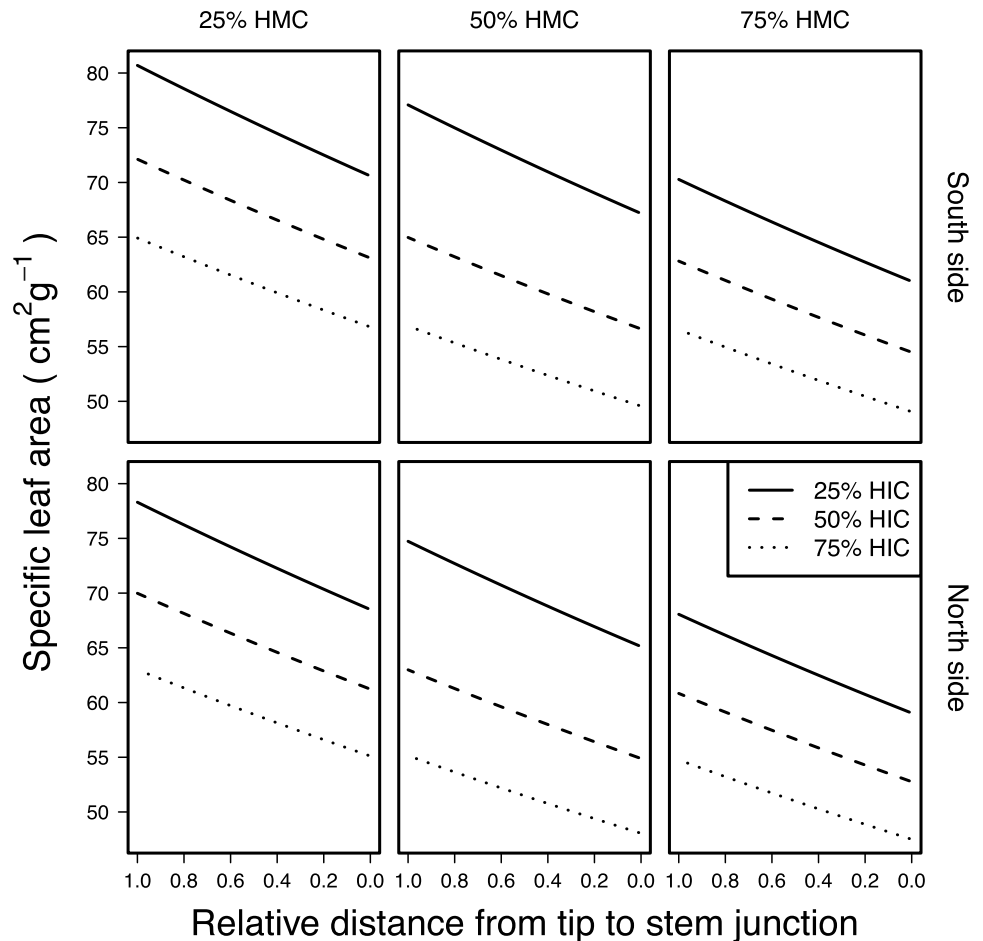
Horizontal distribution of leaf area along branches

Across binning schemes and PDFs, RMSE and MAB reached local minimums with 13 bins. When fitting distribution models for aggregated estimates of LA along the branch lengths, the right-truncated two-parameter Weibull distribution had a marginally better RMSE, but higher MAB than the other PDFs (Table 5). Across all branches, maximum likelihood parameter estimates for Weibull kurtosis (η)

had a mean of 0.672 ± 0.169 and range of 0.316–1.411 and Weibull skew (β) had a mean of 2.990 ± 0.700 and range of 1.432–5.189.

Visual comparison of the fitted Weibull curve to the binned leaf area measurements revealed that Weibull curves fitted horizontal distribution of leaf area better on some branches than others (Fig. 2). Standard error of the Weibull model appeared to be normally distributed along the length of the branch and peaked in the eighth bin. There was no

Table 5 Fit statistics for PDFs

Model (13 bins)	RMSE[a] (mm^2)	MAB[b] (mm^2)
Weibull (right-truncated) (Eq. 1)	92.34	62.79
Beta (Eq. 2)	92.52	62.38
Johnson's S_B (Eq. 3)	92.60	62.44
Weibull (no truncation) (Eq. 1)	94.10	63.74
Weibull (left-truncated) (Eq. 1)	118.43	81.41

[a] Root mean squared error

[b] Mean absolute bias

apparent directional bias along the length of the branch. By bin, absolute bias was strongly correlated with LA ($p < 10^{-6}$; $F = 118.69$; $R^2 = 0.908$).

A total of 42 different models of a variety of forms were fit to the Weibull kurtosis (η) parameter estimates and compared (Online Resource 4). A mixed power and exponential function of HBLC, TBL, RDIC, and a dummy variable for the SW quadrant (Eq. 5) had the highest likelihood, lowest AIC and RMSE, and highest generalized and adjusted fixed and combined fixed and random R^2 among models tested. Equation (5) had the form

$$\eta = h_0 \, \text{HBLC}^{h_1 + q_1 SW} \, \text{TBL}^{h_2 + \omega_j} \, e^{h_3 \text{RDIC}} \tag{5}$$

where h_0, h_1, h_2, h_3, and q_1 are parameters (Table 6), ω_j is the random effect of tree j on total branch length, and SW is a dummy variable for whether the branch was in the southwest quadrant. The inclusion of a factor for whether the branch was in the southwest quadrant significantly improved the model fit over a base model (Eq. 86 in Online Resource 4; $\chi^2 = 6.15$; $df = 1$; $0.01 < p < 0.025$). Inclusion of the random effect ω_j did not improve the R^2 of the kurtosis model compared to a model with only fixed effects (Table 7).

A total of 16 different models of a variety of forms were fit to the skew (β) parameter estimates and compared (Online Resource 5). A power series function of RDIC and BD (Eq. 6) had the highest likelihood, lowest AIC and RMSE, and highest generalized and adjusted fixed and combined fixed and random R^2 among models tested. Equation (6) had form

$$\beta = (h_4 + \omega_j') RDIC^{h_5} (BD/10)^{h_6} \tag{6}$$

Fig. 2 Fitted Weibull curve and actual binned foliage measurements from four branches from the tallest tree in the dataset[†] for NW branches in the lower (**a**) and upper (**b**) crown and SW branches in the lower (**c**) and upper crown (**d**)[‡] [†](UI 217 Tree 4): DBH = 117.8 mm; TH = 1295.4 cm; HBLC = 240.8 cm. [‡]**a**: RDIC = 0.74; TBL = 191 cm; BD = 10.6 mm. **b** RDIC = 0.19; TBL = 52 cm; BD = 5.1 mm. **c** RDIC = 0.73; TBL = 277 cm; BD = 20.6 mm. **d** RDIC = 0.26; TBL = 141 cm; BD = 10.3 mm
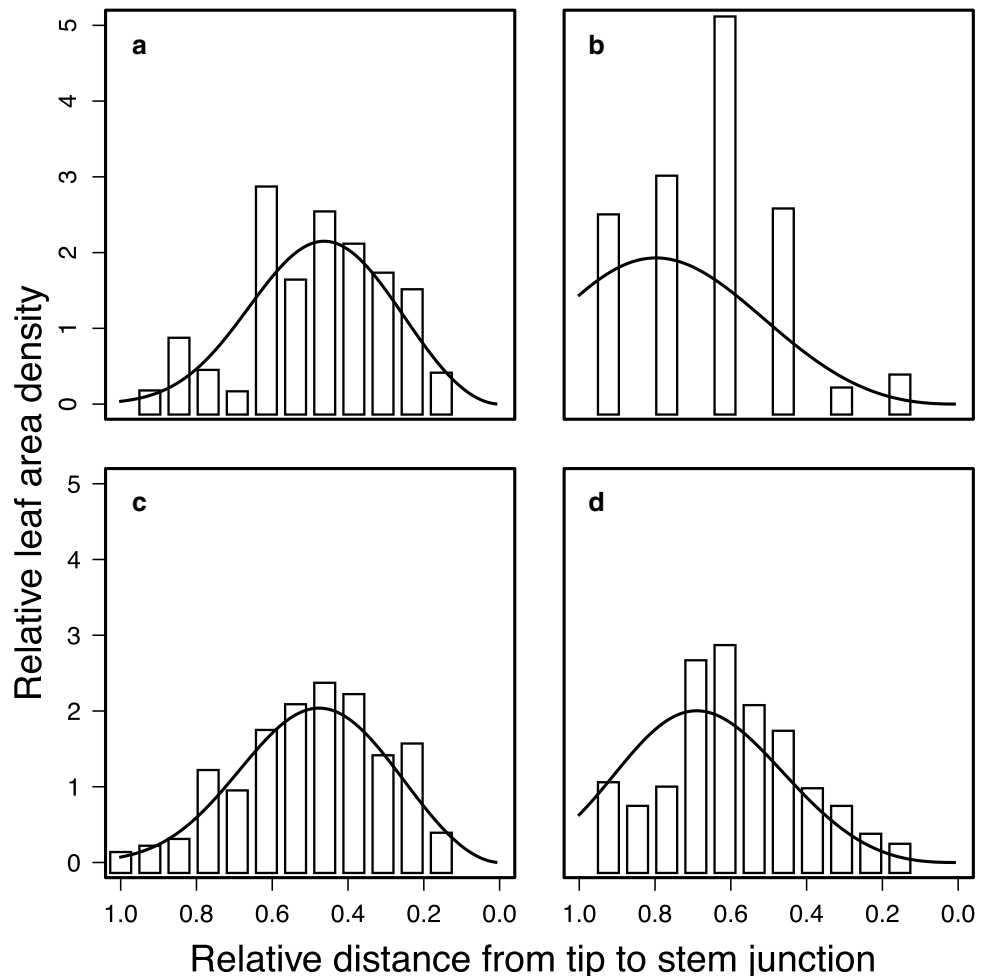
Table 6 Parameter estimates for horizontal Weibull skew and kurtosis models

Model	Parameter	Estimate	SE fixed[a]	SD random[b]	p
Weibull kurtosis (η) (Eq. 5)	h_0	3.395	1.158	NA[c]	0.005
	h_1	−0.069	0.030	NA	0.024
	h_2	−0.254	0.074	0	0.001
	h_3	−0.261	0.121	NA	0.035
	q_1	0.117	0.051	NA	0.026
Weibull skew (β) (Eq. 6)	h_4	2.513	0.139	0.221	0.000
	h_5	−0.207	0.051	NA	0.000
	h_6	0.162	0.075	NA	0.034

[a]Standard error for fixed effects

[b]Standard deviation for random effects for site

[c]Parameter did not include random effects

Table 7 Fit statistics for SLA and horizontal LA distribution parameter models

Model Equation	LL[a]	AIC[b]	RMSE[c]	Adjusted R^2		Generalized R^2	
				Fixed	Fixed + rand	Fixed	Fixed + rand
SLA (Eq. 4)	−715.53	3447.05	7.7200	0.569	0.803	0.573	0.805
Kurtosis (η) (Eq. 5)	50.56	−87.13	0.1325	0.346	0.346	0.378	0.378
Skew (β) (Eq. 6)	−81.11	172.22	0.5952	0.105	0.319	0.127	0.335

[a]Log-likelihood

[b]Akaike's information criterion

[c]Root mean squared error

where h_4, h_5, and h_6 are parameters (Table 6) and ω_j' is the random effect of tree j. Based on the maximum likelihood estimates for the parameters of the selected models fit to Weibull parameter estimates, the kurtosis (η) parameter decreased with RDIC, HBLC, and TBL, and was higher on branches in the southwest (SW) quadrant. Skew (β) decreased with RDIC and increased with BD (Table 6; Fig. 3).

In simple linear models, TBL was positively correlated with RDIC ($F = 38.02$; $df_1 = 1$; $df_2 = 82$; $p = 2.51E-8$; $R^2 = 0.3168$), and so was BD ($F = 20.98$; $df_1 = 1$; $df_2 = 82$; $p = 1.64E-5$; $R^2 = 0.2037$). When linear models are applied to predict TBL and BD from RDIC quantiles for estimation of horizontal leaf area distribution across absolute branch length with Eqs. (5) and (6), leaf area peaks at decreasing RPAB and increasing DAB with increasing RDIC (Fig. 3).

Discussion

Specific leaf area

The average SLA of 64 cm^2 g^{-1} reported here is considerably lower than the range of 100–140 cm^2 g^{-1} reported previously for *L. occidentalis* and other *Larix* spp., (Higgins et al. 1987; Kloeppel et al. 1998; Clawges et al. 2007; Fellner
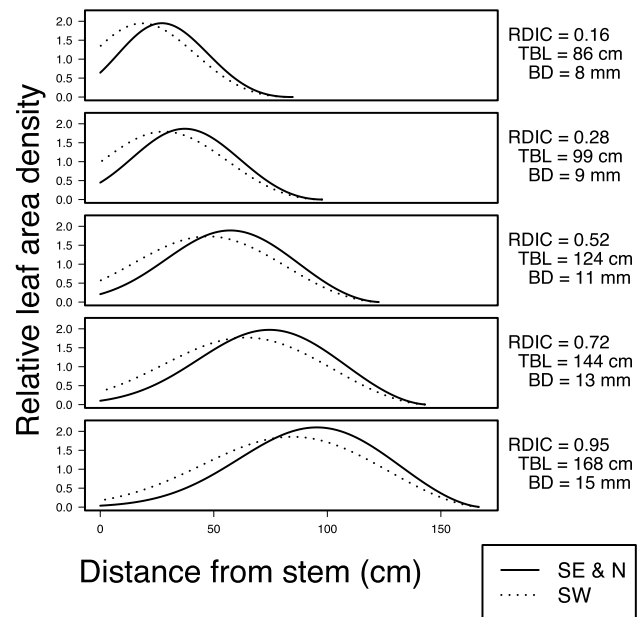

Fig. 3 Predicted horizontal distribution of percent crown leaf area by quadrant (SW vs others) at median height to base of the live crown (HBLC), minimum, first, second, and third quartile, and maximum relative depth of branch in the crown (RDIC), and corresponding expected branch length (TBL) and diameter (BD) predicted from linear models[†]. [†]TBL = 69.326 + 104.473RDIC BD = 6.689 + 8.615RDIC

et al. 2016). Our values are within the range observed in 4-year-old *L. occidentalis* seedlings across a light gradient reported previously (Chen and Klinka 1998). SLA may increase with age due to changing light conditions in the crown and canopy over the course of tree and stand development, potentially explaining differences between our values and those reported from mature trees. Other studies have reported very high SLA of 100–200 cm^2 g^{-1} for *Larix decidua* Mill., and 200–275 cm^2 g^{-1} for other *Larix* spp. (Richards and Bliss 1986; Matyssek and Shulze 1987). Higher SLA in *Larix* spp. relative to evergreen conifers fits the trend of decreasing SLA with increased leaf lifespan (Reich et al. 1997).

The well-supported negative correlation between leaf lifespan and SLA has been demonstrated to underpin a number of other correlations between metabolism and N and P content observed across the leaf economics spectrum (Wright et al. 2004; Osnas et al. 2013). As foliage ages, SLA and rate of photosynthesis per unit mass investment decrease together (Gower et al. 1993). Thus, short-lived foliage yields a greater relative photosynthetic return on investment in limiting organic and mineral resources (Ellsworth and Reich 1993; Bond et al. 1999). Efficiency of resource use by the deciduous foliage of *L. occidentalis* may partly contribute to the high growth rates and growth efficiency of *Larix* spp., whose crowns accumulate foliage much more slowly with increasing stem diameter than other species (Forrester et al. 2017; Williams et al. 2017).

The negative correlations of SLA with height to the middle of the crown, height of the branch in the crown, and distance along the branch from the stem observed for *L. occidentalis* in this study (Table 4; Fig. 1) are consistent with studies of many other species (Van Hees and Bartelink 1993; Ishii et al. 2002; Sellin and Kupper 2006; Temesgen and Weiskittel 2006). In contrast to species where SLA is negatively correlated with light availability (Chen et al. 1996), our observations of within-crown SLA variation are consistent with the hydraulic resistance and gravitational water potential hypothesis. Chen and Klinka (1998) did not find a significant relationship between SLA and light availability in *L. occidentalis* seedlings. Variation in SLA not accounted for by our model may be due to additional extrinsic and/or intrinsic factors.

To the best knowledge of the authors, only one other study has investigated the influence of cardinal branch direction on SLA, and did not report a significant effect for either *Pseudotsuga menziesii* var. *menziesii* (Mirb.) Franco or hybrid *Picea* (Weiskittel et al. 2008). Here, we report significantly higher SLA on the south side of crowns of *L. occidentalis* after accounting for other variables (Table 4). The result of highest SLA on the best-lit portion of the crown was unexpected. In general, sun leaves have lower SLA than shade leaves. The south side is more illuminated, so our results

indicate a lack of plasticity of SLA to light availability in *L. occidentalis*, as reported for other species (Niinemets and Kull 1994; Chen et al. 1996). The observed effect of branch quadrant on SLA, though statistically significant, was small (Table 4).

Capacitance and hydraulic conductance were not likely to be limiting factors during leaf expansion for the juvenile trees in our study, which grew on sites with significant ash deposition and high moisture holding capacity, and were sampled in a year with higher than average precipitation. Higher SLA observed on the south side of the trees relative to the less irradiated north side (Fig. 1) may have been a consequence of decreased transpiration due to higher vapor pressure deficit, and in turn, higher turgor pressure during leaf expansion (Tardieu et al. 1999). However, measurements of stomatal closure, gas exchange, and water potential, as well as environmental parameters would have been required to support this physiological inference. Furthermore, there may be alternative explanations for our unexpected result due to factors we have failed to consider (i.e., other than light and hydraulic constraints).

Horizontal distribution of leaf area

The right-truncated Weibull function fit horizontal distribution of foliage along branches of *L. occidentalis* as well as or better than it has for other species (Table 5). The distribution of leaf area along individual branches varied greatly within individual trees (Fig. 2). Consequently, the kurtosis and skew models had low R^2 values (Table 7). In addition to irregularly-distributed sunflecks in the crown from the clumped allocation of foliage on short shoots characteristic of *Larix* spp., extrinsic factors that were not measured or tested could have contributed to variation, such as defoliation due larch needle blight (*Hypodermella laricis* Tub.), which was present in some of the foliage samples.

Here, we report a significant effect of cardinal branch position on horizontal leaf area distribution (Fig. 3). Zhao and Wang (2004) found a significant difference in branch length and bifurcation ratio between southern and northern sides of the crown in *Larix chinensis* Beissn., which taken together with our findings suggests crown morphology is plastic to level of light and/or solar heat radiation in the genus *Larix*. Given our site location in the northern hemisphere and on the western slope of the Rocky Mountains, the southwest quadrant of the tree crown should receive more light and heat than the other quadrants.

In general, a proximally shifted distribution of leaf area may reduce water loss, or it may sustain transpiration and thus higher rates of photosynthesis late in the season under high irradiance by allowing the stomata to remain open. Under this hypothesis, lower rates of photosynthesis due to the closing of stomata would then prevent foliage retention

on the more distal portions of the branches, where vapor deficit is highest. Furthermore, water potential decreases with distance along the branch from the main stem, limiting the amount of leaf expansion. The peak in leaf area near the middle of the branch—the "sweet spot"—in juvenile *L. occidentalis* may reflect a balancing act between hydraulic and light constraints. Foliage cannot fix enough carbon to support itself proximal to the branch midpoint, but also encounters hydraulic stress near the branch tips. The present study was limited to juvenile trees between 10- and 14-years-old, and also did not capture variation in SLA and horizontal leaf area distribution across the full range of environmental conditions in which *L. occidentalis* grows.

Conclusions

We applied a non-linear mixed effect modelling approach to SLA and horizontal distribution of leaf area along branches of western larch. SLA decreased with increasing branch height and distance along branches away from the stem. Unlike other studies, the peak of SLA depended on cardinal branch position. Unexpectedly, SLA was higher in the more illuminated south side of the tree. Peak leaf area was shifted closer to the stem in the southwest quadrant. We have presented a physiological interpretation of the intrinsic variation observed from our models as a hypothesis to explain our results: namely, that hydraulic constraints drive the spatial variation of SLA and leaf area in western larch crowns. However, further research incorporating physiological measurements is needed to properly test this hypothesis, and other explanations are possible. In combination with models developed for vertical distribution of foliar biomass (Williams et al. 2017), the models developed here could be extended to include the effect of extrinsic factors such as site or climate on canopy development in *L. occidentalis*.

Compliance with ethical standards

Conflict of interest The authors declare that they have no conflict of interest.

References

Anfodillo T, Rento S, Carraro V, Furlanetto L, Urbinati C, Carrer M (1998) Tree water relations and climatic variations at the alpine timberline: seasonal changes of sap flux and xylem water potential in *Larix decidua* Miller, *Picea abies* (L.) Karst. and *Pinus cembra* L. Ann Sci Forest 55(1–2):159–172

Arno SF, Smith HY, Krebs MA (1997) Old growth ponderosa pine and western larch stand structures: influence of pre-1900 fires and fire exclusion. INT-RP-495. US Dept of Agriculture, Intermountain Research Station

Bond BJ, Farnsworth BT, Coulombe RA, Winner WE (1999) Foliage physiology and biochemistry in response to light gradients in conifers with varying shade tolerance. Oecologia 120(2):183–192

Buckley DS, Zasada JC, Tappeiner IIJC, Stone DM (1997) Plant morphological characteristics as a tool in monitoring response to silvicultural activities. In: Communicating the role of silviculture in managing the national forests: Proceedings of the National Silviculture Workshop. Warren, PA, 19–22 May 1997. GTR-NE-238. Northeast Forest Experimental Station, Forest Service, US Dept of Agriculture

Chabot BF, Hicks DJ (1982) The ecology of leaf life spans. Annu Rev Ecol Syst 13(1):229–259

Chen HY, Klinka K (1998) Survival, growth, and allometry of planted *Larix occidentalis* seedlings in relation to light availability. Forest Ecol Manag 106(2):169–179

Chen HY, Klinka K, Kayahara GJ (1996) Effects of light on growth, crown architecture, and s pecific leaf area for naturally established *Pinus contorta* var. *latifolia* and *Pseudotsuga menziesii* var. *glauca* saplings. Can J For Res 26(7):1149–1157

Clawges R, Vierling L, Calhoon M, Toomey M (2007) Use of a ground-based scanning lidar for estimation of biophysical properties of western larch (*Larix occidentalis*). Int J Remote Sens 28(19):4331–4344

Ellsworth DS, Reich PB (1993) Canopy structure and vertical patterns of photosynthesis and related leaf traits in a deciduous forest. Oecologia 96(2):169–178

Fellner H, Dirnberger GF, Sterba H (2016) Specific leaf area of European Larch (*Larix decidua* Mill.). Trees 30:1237–1244

Forrester DI, Tachauer IHH, Annighoefer P, Barbeito I, Pretzsch H, Ruiz-Peinado R, Stark H, Vacchiano G, Zlatanov T, Chakraborty T, Saha S (2017) Generalized biomass and leaf area allometric equations for European tree species incorporating stand structure, tree age and climate. For Ecol Manag 396:160–175

Goudie JW, Parish R, Antos JA (2016) Foliage biomass and specific leaf area equations at the branch, annual shoot and whole-tree levels for lodgepole pine and white spruce in British Columbia. Forest Ecol Manag 361:286–297

Gower ST, Reich PB, Son Y (1993) Canopy dynamics and aboveground production of five tree species with different leaf longevities. Tree Physiol 12(4):327–345

Gulmon SL, Chu CC (1981) The effects of light and nitrogen on photosynthesis, leaf characteristics, and dry matter allocation in the chaparral shrub, *Diplacus aurantiacus* Oecologia 49(2):207–212

Higgins SS, Black RA, Radamaker GK, Bidlake WR (1987) Gas exchange characteristics and water relations of *Larix occidentalis*. Can J For Res 17(11):1364–1370

Horn HS (1971) The Adaptive Geometry of Trees. Princeton University Press, Princeton

Ibrahim L, Proe MF, Cameron AD (1998) Interactive effects of nitrogen and water availabilities on gas exchange and whole-plant carbon allocation in poplar. Tree Physiol 18:481–487

Ishii H, Ford ED, Boscolo ME, Manriquez AC, Wilson ME, Hinckley TM (2002) Variation in specific needle area of old-growth Douglas-fir in relation to needle age, within-crown position and epicormic shoot production. Tree Physiol 22(1):31–40

Jurik TW (1986) Temporal and spatial patterns of specific leaf weight in successional northern hardwood tree species. Am J Bot 73(8):1083–1092

Kershaw JA, Maguire DA (1996) Crown structure in western hemlock, Douglas-fir, and grand fir in western Washington: horizontal distribution of foliage within branches. Can J For Res 26:128–142

Kloeppel BD, Gower ST, Treichel IW, Kharuk S (1998) Foliar carbon isotope discrimination in *Larix* species and sympatric evergreen conifers: a global comparison. Oecologia 114(2):153–159

Marshall JD, Monserud RA (2003) Foliage height influences specific leaf area of three conifer species. Can J For Res 33:164–170

Matyssek R, Schulze ED (1987) Heterosis in hybrid larch (*Larix decidua* × *leptolepis*). I. The role of leaf characteristics. Trees 1(4):219–224

McClelland BR, Frissell SS, Fischer WC, Halvorson CH (1979) Habitat management for hole-nesting birds in forests of western larch and Douglas-fir. J For 77(8):480–483

Myers BJ, Benyon RG, Theiveyanathan S, Smith CJ, Smith CJ, Falkiner RA (1998) Response of effluent-irrigated *Eucalyptus grandis* and *Pinus radiata* to salinity and vapor pressure deficits. Tree Physiol 18:565–573

Niinemets Ü (1996) Plant growth-form alters the relationship between foliar morphology and species shade-tolerance ranking in temperate woody taxa. Vegetatio 124(2):145–153

Niinemets Ü, Kull K (1994) Leaf weight per area and leaf size of 85 Estonian woody species in relation to shade tolerance and light availability. For Ecol Manag 70:1–10

Niinemets Ü, Kull O (1995) Effects of light availability and tree size on the architecture of assimilative surface in the canopy of *Picea abies*: variation in shoot structure. Tree Physiol 15(12):791–798

Oliver CD, Larson BC (1990) Forest stand dynamics. McGraw-Hill, New York

Oren R, Schulze ED, Matyssek R, Zimmermann R (1986) Estimating photosynthetic rate and annual carbon gain in conifers from specific leaf weight and leaf biomass. Oecologia 70(2):187–193

Osnas JL, Lichstein JW, Reich PB, Pacala SW (2013) Global leaf trait relationships: mass, area, and the leaf economics spectrum. Science 340(6133):741–744

Perrin PM, Mitchell FJ (2013) Effects of shade on growth, biomass allocation and leaf morphology in European yew (*Taxus baccata* L.). Eur J Forest Res 132(2):211–218

Phillips JG, Riha SJ (1993) Canopy development and solar conversion efficiency in *Acacia auriculiformis* under drought stress. Tree Physiol 12:137–149

Pinheiro J, Bates D, DebRoy S, Sarkar D, Core Team R (2017) nlme: linear and nonlinear mixed effects models. R package version 3.1-131. https://CRAN.R-project.org/package=nlme. Accessed 18 Apr 2017

R Core Team (2017) R: a language and environment for statistical computing. R Foundation for Statistical Computing, Vienna, Austria. https://www.R-project.org. Accessed 18 Apr 2017

Rehfeldt GE, Jaquish BC (2010) Ecological impacts and management strategies for western larch in the face of climate-change. Mitig Adapt Strat Gl 15:283–306

Reich PB, Walters MB, Ellsworth DS (1997) From tropics to tundra: Global convergence in plant functioning. PNAS 94(25):13730–13734

Richards JH, Bliss LC (1986) Winter water relations of a deciduous timberline conifer. Larix lyallii Parl Oecol 69(1):16–24

Schmidt WC, Shearer RC (1990) Western larch (Larix occidentalis). In: Burns RM, Honkala B (eds) Silvics of North America, vol 1. Conifers. Agricultural Handbook 654. Forest Service, US Dept of Agriculture, Washington

Scott G, Mahalovich MF, Rinehart S, Krueger J (2013) Reforestation-revegetation climate change primer for the northern region: incorporating climate change impacts into reforestation and revegetation prescriptions. Forest Service, US Dept of Agriculture. http://ecoadapt.org/data/documents/Reforestation-Revegetation_Primer_Final.pdf. Accessed 18 Apr 2017

Sellin A, Kupper P (2006) Spatial variation in sapwood area to leaf area ratio and specific leaf area within a crown of silver birch. Trees 20(3):311–319

Stenberg P, Smolander H, Kellomäki S (1993) Description of crown structure for light interception models: angular and spatial distribution of shoots in young Scots pine. Stud For Suec 191:43–50

Stenberg P, Kuuluvainen T, Kellomäki S, Grace JC, Jokela EJ, Gholz HL (1994) Crown structure, light interception and productivity of pine trees and stands. Ecol Bulletins 43:20–34

Tardieu F, Granier C, Muller B (1999) Modelling leaf expansion in a fluctuating environment: are changes in specific leaf area a consequence of changes in expansion rate? New Phytol 143:33–43

Temesgen H, Weiskittel AR (2006) Leaf mass per area relationships across light gradients in hybrid spruce crowns. Trees 20(4):522–530

Temesgen H, LeMay VM, Cameron IR (2003) Bivariate distribution functions for predicting twig leaf area within hybrid spruce crowns. Can J For Res 33:2044–2051

Van Hees AFM, Bartelink HH (1993) Needle area relationships of Scots pine in the Netherlands. Forest Ecol Manag 58(1):19–31

Wang YP, Jarvis PG, Benson ML (1990) Two-dimensional needle-area density distribution within the crowns of *Pinus radiata*. Forest Ecol Manag 32:217–237

Weiskittel AR, Temesgen H, Wilson DS, Maguire DA (2008) Sources of within- and between-stand variability in specific leaf area of three ecologically distinct conifer species. Ann Forest Sci 65:103

Weiskittel AR, Kershaw JA, Hofmeyer PV, Seymour RS (2009) Species differences in total and vertical distribution of branch- and tree-level leaf area for the five primary conifer species in Maine, USA. Forest Ecol Manag 258:1695–1703

Williams GM, Nelson AS, Affleck DL (2017) Vertical distribution of foliar biomass in western larch (*Larix occidentalis*). Can J For Res 48(1):42–57

Wright IJ, Reich PB, Westoby M, Ackerly DD, Baruch Z, Bongers F, Flexas J et al (2004) The worldwide leaf economics spectrum. Nature 428(6985):821–827

Xu M, Harrington TB (1998) Foliage biomass distribution of loblolly pine as affected by tree dominance, crown size, and stand characteristics. Can J For Res 28:887–892

Zhao X, Wang X (2004) Study on branching pattern plasticity of *Larix chinensis*. Acta Bot Boreali-Occidentalia Sinica 25(1):113–117